Progress in Engineering Science 1 (2024) 100002

Contents lists available at ScienceDirect

Progress in Engineering Science

journal homepage: www.sciencedirect.com/journal/progress-in-engineering-science

Second law efficiency of air-cooled refrigeration compressors

Mohammad Arqam[a,*], Amir Jahangiri[b], Mark Mitchell[b], Nick S. Bennett[a], Peter Woodfield[c]

[a] School of Mechanical and Mechatronic Engineering, University of Technology Sydney, Broadway, NSW, Australia
[b] Unicla International Ltd., Ormeau, Queensland, Australia
[c] School of Engineering and Built Environment, Griffith University, Australia

ARTICLE INFO

Keywords:
Isentropic efficiency
Refrigeration compressor performance
Swashplate compressor

ABSTRACT

Isentropic efficiency is a common performance measure for compressors and is useful for modelling the behaviour of real compressors in relation to discharge temperature or required mechanical power input. However, it has a weakness in that a basic assumption in the calculation is that the real compressor is adiabatic. If significant heat transfer from the compressor to the outside environment occurs, then the adiabatic assumption is invalid, but the negative effects of internal entropy generation are reduced, and in principle it is possible to have a measured isentropic 'efficiency' greater than 100%, which, while counterintuitive, is highly desirable. We practically demonstrate this effect with an air-cooled swashplate compressor and propose that for cases of intentional compressor cooling, the simple definition for isentropic efficiency is retained as a performance measure but renamed to isentropic performance coefficient (IPC).

1. Introduction

Refrigeration compressors are typically assessed using both the first and second laws of thermodynamics. The second law of thermodynamics establishes the concept of energy quality, and it can be utilized to evaluate the degradation of energy quality that occurs during a process or cycle. However, compared to first law (energy) analysis, second law (exergy) analysis offers a more precise and effective approach for identifying areas of inefficiency. The insights gained from exergy analysis can be used to evaluate and enhance the performance of refrigeration compressors, making it a valuable tool for improving their efficiency and effectiveness.

High performance reciprocating compressors are widely accepted in the automobile industry due to their compact structure, small size, light weight, low cost, and better thermal comfort inside the vehicle cabin [1–3]. Reciprocating compressor performance in terms of efficiency has been investigated by many researchers through incorporating mathematical models. For example, a methodology for thermodynamic modelling of reciprocating compressors including the working process inside the cylinder was presented by Sun and Ren [4]. Farzaneh et al. [5–7] presented a thermodynamic model to analyse the effects of natural gas composition on the compressed natural gas refrigeration compressor performance. Moreover, a thermodynamic analysis on single stage reciprocating expansion engine was carried out by the same group [8,9]. A comprehensive analytical model based on kinematics, compression process and friction power loss was developed in reference [10]. An electric motor model for hermetic reciprocating compressors was introduced by Dutra et al. [11] for more accurate prediction of compressor performance in terms of efficiency and temperature distribution. Thermodynamic performance evaluation of reciprocating compressors was also carried out by Wang et al. [12] and Zhao et al. [13]. One used an m-θ diagram while the other investigation involved transient temperature measurement based on a two-thermocouple probe method. Elhaji et al. [14] conducted a numerical study of a two-stage reciprocating compressor, which led to the expansion of diagnostic features for predictive condition monitoring. Winandy et al. [15] developed a simplified model of an open-type reciprocating compressor, which showed the main processes that influenced the refrigerant mass flow rate, compressor power, and discharge temperature. Ndiaye and Bernier [16] also created a dynamic model of a hermetic reciprocating compressor in on-off cycling operation.

Some researchers have focused on parametric studies for evaluating compressor performance to aid design and development of high efficiency refrigeration compressors. Stouffs et al. [17] presented a methodology for investigating compressor performance considering nine physically meaningful dimensionless parameters (five main and four secondary). The effect of geometry, valves, motor and working conditions on the compressor performance was discussed by Rigola et al. [18]. Clearance ratio and the friction factor have considerable influence on volumetric and isentropic efficiencies as reported by Castraing et al.

* Corresponding author.
E-mail address: Mohammad.Arqam@uts.edu.au (M. Arqam).

https://doi.org/10.1016/j.pes.2024.100002
Received 17 February 2024; Received in revised form 27 March 2024; Accepted 29 March 2024

Nomenclature

η_s	isentropic efficiency
$\dot{W}_s$	ideal work input, J/kg
$\dot{W}_a$	actual mechanical work input to compressor, J/kg
$\dot{m}$	mass flow rate, kg/s
h_1	specific enthalpy at suction line, J/kg
h_{2a}	specific enthalpy at discharge line, J/kg
h_{2s}	isentropic specific enthalpy at discharge line, J/kg
$\dot{Q}_{out}$	heat transfer rate, W
P_{suc}	suction pressure, Pa
P_{dis}	discharge pressure, Pa
h_{suc}	enthalpy per unit mass at compressor suction, J/kg
h_{dis}	enthalpy per unit mass at compressor discharge, J/kg
$h_{dis,\ isen}$	isentropic enthalpy per unit mass at compressor discharge, J/kg
T_{suc}	suction temperature, ˚C
T_{dis}	discharge temperature, ˚C
s_{suc}	specific entropy at suction, J/kg. K
P_{comp}	power consumption, W
T_{amb}	ambient temperature, ˚C
ds	change in specific entropy, J/kg. K
T_{wall}	cylinder inside wall temperature, ˚C
W_c	compression work, J/kg
Q_H	heat rejected from the condenser, J/kg
Q_L	cooling capacity, J/kg
COP	coefficient of performance
RPM	revs per minute

[19]. Fluid dependent efficiencies can be predicted using a differential compressor model introduced by Roskosch et al. [20]. Posch et al. [21] and Navarro et al. [22] performed numerical analysis based on thermal loss to predict reciprocating compressor performance. Farzaneh-Gord et al. [23] optimized the design parameters of a reciprocating air compressor thermodynamically by developing a mathematical model based on mass conservation, the first law, and the ideal gas assumption to study the performance of reciprocating compressors.

The researchers mentioned above utilized the first law of thermodynamics as a fundamental tool for modelling. The second law of thermodynamics was also employed to assess the performance of reciprocating compressors. McGovern and Harte [24] explored compressor performance by employing the second law, which characterizes non-idealities as exergy destruction rates caused by losses due to friction, irreversible heat transfer, fluid throttling, and irreversible fluid mixing. The study also identified and quantified defects in the use of a compressor's shaft power. Aprea et al. [25] conducted research that detected the optimum frequency for variable speed compressors in terms of exergy, energy, and economy. Additionally, Bin et al. [26] investigated the thermal performance of reciprocating compressors with stepless capacity control systems. Their experimental setup demonstrated the successful operation of the compressor with the designed stepless capacity control system. Morriesen and Deschamps [27] conducted an experimental investigation of transient fluid and superheating in the suction chamber of a refrigeration reciprocating compressor. Furthermore, Yang et al. [28] simulated a semi-hermetic CO_2 reciprocating compressor comprehensively.

The literature reviewed above indicates that the application of second law analysis in predicting the performance of refrigeration compressors includes parameters such as design characteristics, shaft power, internal heat transfer, friction losses, and fluid dynamics inside the compressor. However, few studies have discussed the second law efficiency by considering external cooling, which involves significant heat transfer from the compressor to the surrounding environment. While considering the importance of heat exchange with the surroundings, this study aims to practically demonstrate the impact of intentional cooling on the isentropic efficiency of refrigeration compressors.

It is well known that external cooling is desirable to improve the performance of a compressor. The ideal device is the so-called 'isothermal compressor' where work input is significantly lower than the ideal 'isentropic compressor' (e.g. Cengel et al. [29]). For the compression of refrigerants (especially with fixed-displacement mechanisms), isothermal compression is not a practical target due to the undesired presence of liquid in the two-phase mixture and the simple principle that the temperature in the condenser must be higher than the air temperature of the surrounding environment for the condenser to reject heat. Nevertheless, cooling of the compressor reduces the discharge temperature and therefore the load on the condenser, which is desirable.

The isentropic efficiency of a compressor is defined as:

$$\eta_s = \frac{\dot{W}_s}{\dot{W}_a} \approx \frac{h_{2s} - h_1}{h_{2a} - h_1} \tag{1}$$

where $\dot{W}_s$ and $\dot{W}_a$ are the ideal isentropic work input and actual work input, h is specific enthalpy and suction and discharge lines are labelled 1 and 2, respectively. The expression involving enthalpies is the easiest to measure and assumes no heat transfer to the surroundings. If one includes heat transfer to the surroundings, then the expression becomes:

$$\frac{\dot{W}_s}{\dot{W}_a} = \frac{\dot{m}(h_{2s} - h_1)}{\dot{m}(h_{2a} - h_1) + \dot{Q}_{out}} \tag{2}$$

where $\dot{Q}_{out}$ is the heat transfer rate from the compressor to the surroundings and $\dot{m}$ is the mass flow rate of refrigerant. For measuring performance of a compressor with cooling, Eq. (2) is less convenient because the heat transfer to the surroundings, $\dot{Q}_{out}$ or the mechanical power input, $\dot{W}_a$ are extra parameters that are more difficult to measure in comparison with the discharge temperature. Cengel et al. [29] suggest it is 'meaningless' to report the isentropic efficiency of a compressor with intentional cooling. However, this creates a dilemma for testing and comparing practical devices if we are unable to report the compressor's isentropic efficiency. Moreover, a refrigeration compressor with a lower discharge temperature is certainly a better compressor. Since, for a compressor, it is desirable to both lower h_{2a} and increase $\dot{Q}_{out}$, we propose that the isentropic efficiency based on enthalpies is still a practical, convenient, and meaningful performance measure for intentionally cooled compressors. To avoid ambiguities and concerns about the 'efficiency' exceeding 100%, we suggest that for intentionally cooled compressors, the apparent isentropic efficiency based on enthalpies be relabelled as:

$$Apparent \quad \eta_s = IPC \equiv \frac{h_{2s} - h_1}{h_{2a} - h_1} \tag{3}$$

where *IPC* stands for isentropic performance coefficient. In the case of an adiabatic compressor, *IPC* becomes identical to the isentropic efficiency. For an externally cooled compressor, *IPC* improves with an increase in cooling to the surroundings. For diabatic compressors, Zou et. al [30] call the efficiency evaluated by Eq. (3) the 'apparent efficiency'. Their study involves heat transfer into the compressor from a neighboring gas turbine rather than intentional cooling.

Fig. 1 illustrates how the isentropic efficiency can appear to exceed 100% if cooling to the surroundings takes place. The rectangle represents the boundary of the compressor. Fig. 1a) is an adiabatic compressor with an isentropic efficiency of 90%. This case fits well with the definition of isentropic efficiency. Fig. 1b) shows the same

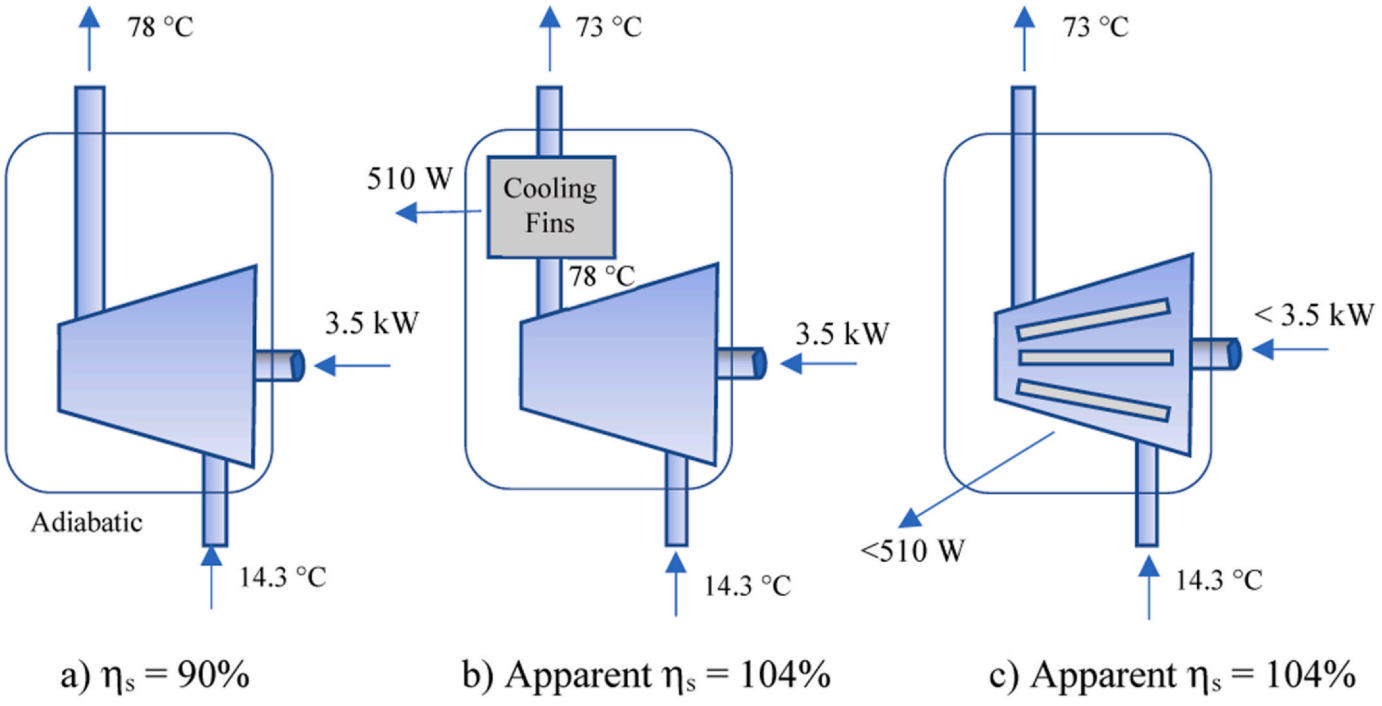

Fig. 1. Illustration of how the apparent isentropic efficiency can exceed 100% if the compressor has cooling to the surroundings.

compressor with external cooling fins on the flow passage connecting the compressor discharge to the discharge line. The values in the figure correspond to conditions relevant to the compressor tested in this study (as listed in Table 1). If the enthalpy at the exit is calculated based on the lower discharge temperature of 73 ˚C, the isentropic efficiency based on enthalpies will become 104%. Based on Eq. (2), the isentropic efficiency for the cases shown in Figs. 1a) and 1b) will be the same, since the mechanical power input is the same. We argue that the compressor shown in Fig. 1b) performs better than the one in Fig. 1a) since the discharge temperature is lower. Fig. 1c) is better again since heat is removed during the compression process. For the compressor considered in this study, the cooling behaviour will be somewhere between Figs. 1b) and 1c).

2. Experimental setup

An air-cooled 10-cylinder electric swashplate compressor was tested using the set up illustrated in Fig. 2. The key components are a fixed-displacement swash-plate compressor Unicla UP200 (200 ccrev^{-1}), a condenser KYSOR Westran KC90 (capacity performance of 7.6 kW), an evaporator MICRO-BUS BEU-848 L-100 (cooling capacity of 9.4 kW) and a thermal expansion valve (TXV). A drier and an oil separator were also present as auxiliary equipment. A volumetric flow meter located at the exit to the evaporator was used to monitor the flow rate of refrigerant through the circuit. The components used in the experiment were connected through hoses to circulate refrigerant between two separate insulated rooms (evaporator room and the condenser room). 10 kW and 15 kW electric heaters were set to supply heated air in the condenser and evaporator rooms which had dimensions (width × length × height) of 6 m × 6.5 m × 6 m, and 3.5 m × 6 m × 2.7 m, respectively.

The swashplate compressor under consideration has 10 cylinders (5 double-ended pistons) with a diameter of 31 mm, and a maximal power consumption of 3.5 kW. A 4-kW brushless DC motor with a variable frequency drive was used to control the rotational speed of the compressor. The pressure and temperature sensors were installed at the inlet and outlet of the compressor and the power consumed by the compressor was measured. The pressure levels and ratios were controlled by adjusting air-flow rate in the condenser and flow through expansion valve. Temperature and pressure measurements were carried out using 4 terminals PT100 platinum resistance thermometers and electronic pressure transducers. The pressure, temperature sensors and the flow meter were connected to a multi-channel data logger (ALMEMO5690) to send the information to a computer. At the beginning of the experiment, the compressor and pipelines were set to an adequate vacuum condition to remove humidity, air and other contaminants that might affect the overall performance of the system. Subsequently, the system was charged with an appropriate amount of R134a or R404a refrigerant. The corresponding values were recorded every second within the measuring cycle. After steady state was achieved, the data was recorded for 200 min and the averaged values are used for the analysis. For the systematic analysis, different values of suction pressure and temperature were investigated for R134a and R404a refrigerants. The compressor speed was initially held constant at 1800 rpm and then the effect of variation was also investigated. Finally, the isentropic performance coefficient was calculated using

Table 1
Typical measured conditions for the compressor in this study.

Pdis *(Bar)*	P_{suc} *(Bar)*	T_{dis} *(° C)*	T_{suc} *(° C)*	s_{suc} *(kJ/kg.K)*	*hsuc* *(kJ/kg)*	h_{dis} *(kJ/kg)*	$h_{dis,\ isen}$ *(kJ/kg)*	*IPC*
14.75	2.79	73.3	14.3	1.777	411.61	447.65	449.27	1.04 ± 0.09

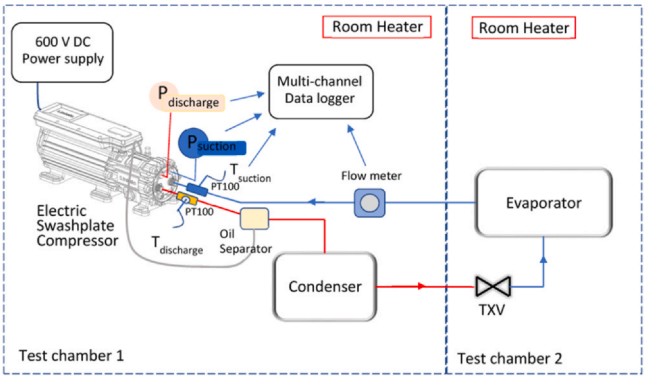

Fig. 2. Schematic of experimental test setup.

measurements at the inlet and outlet of the compressor and the mass flow rate of the refrigerant through employing the REFPROP (Lemmon et al. [31]) database for obtaining enthalpies. The photographs of the experimental setup are shown in Fig. 3.

2.1. Uncertainty in the measurement

The measuring instruments have the following accuracies: PT100 platinum resistance thermometer ± 0.5ºC, refrigerant pressure ± 2% of full-scale reading, refrigerant volume flow rate ± 5%, and compressor rotational speed ± 1% for 1000–3000 rpm, as depicted in Table 2. The DC power supply has an uncertainty estimated at ± 2 V for the 600 V setting. The effect of the uncertainty in the pressure reading on the isentropic efficiency calculated by Eq. (1) is quite significant.

3. Results

3.1. Effect of environment temperature and discharge pressure

Fig. 4 shows the apparent isentropic efficiency as defined by Eq. (3) of the air-cooled swashplate compressor. During testing the temperature of the test chamber was periodically varied by switching the test chamber heaters on and off and allowing outside air to enter. For most of the test, the apparent isentropic efficiency is greater than 100%. During the first 10–15 minutes after starting the compressor, the apparent isentropic efficiency is high. This may be attributed to the extra cooling that the refrigerant experiences as it heats up the metal in the compressor body. The room temperature appears to have only a minor effect on the measured efficiency. Following the reasoning that extra cooling will improve the apparent isentropic efficiency, it is unexpected that the performance measure is higher after 100 minutes when the room temperature is higher on average. This may be due to the lower discharge pressures and temperatures shown in Fig. 5 after 100 minutes and uncertainty in the measurement. From Fig. 4, it is observed that the fluctuations in isentropic efficiency measurements did not allow to define a specific trend different from a constant value.

3.2. Effect of compressor speed

The effect of compressor speed on the isentropic performance coefficient was investigated. The test was performed at constant suction and discharge pressures. As depicted in Table 3, the slower speed leads to increased isentropic performance coefficient by 0.13 due to the reason that slower speed provides enough time for the heat to disperse. The compressor consumed more power at higher speed than at lower rpm.

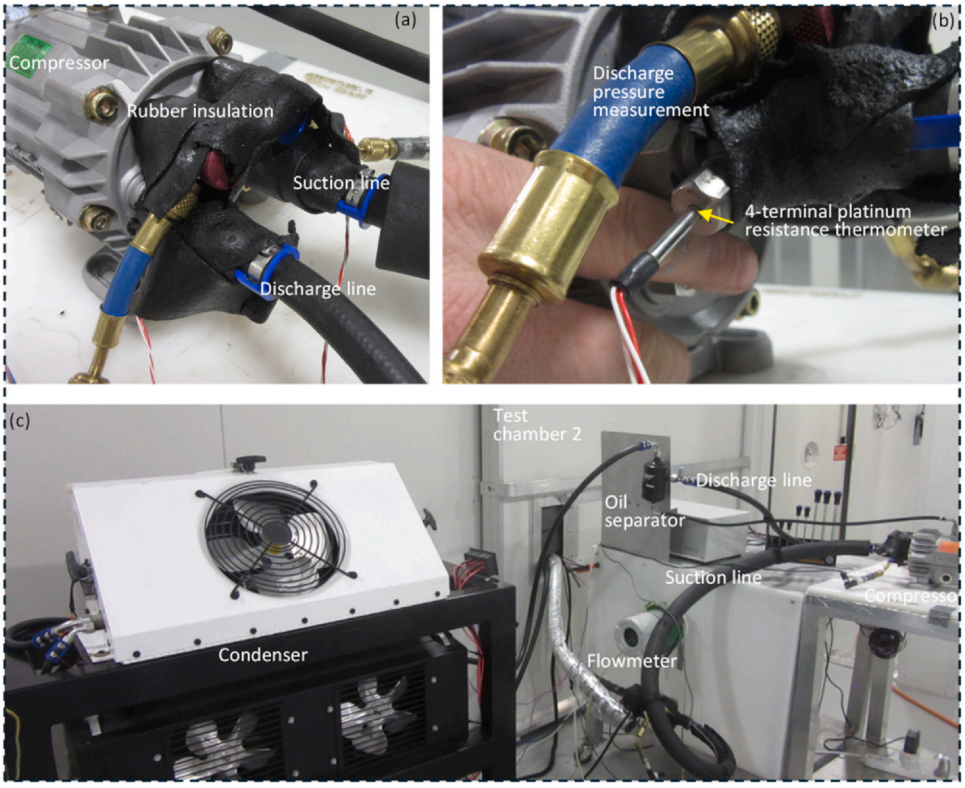

Fig. 3. Photographs of experimental setup. (a) compressor; (b) 4 terminal PT100 platinum resistance thermometers were embedded into the flow lines so that the sensing elements are in direct contact with the refrigerant; (c) condenser and evaporator setup in test chamber 2.

Table 2
Measurement uncertainty.

Instrument	*Variable*	*Accuracy*	*Effect on η_s*
Pressure transducer	Suction Pressure	± 2%	± 6.6%
	Discharge Pressure	± 2%	± 5.5%
PT100 thermometer	Suction Temperature	± 0.5 ºC	± 1.5%
	Discharge Temperature	± 0.5 ºC	± 1.6%
Variable speed drive	Rotational speed	± 1%	-
Coriolis flow meter	Refrigerant flow rate	± 5%	-
DC power supply	Voltage measurement	< 0.5% or 2 V	-
	Total uncertainty in η_s		**± 9%**

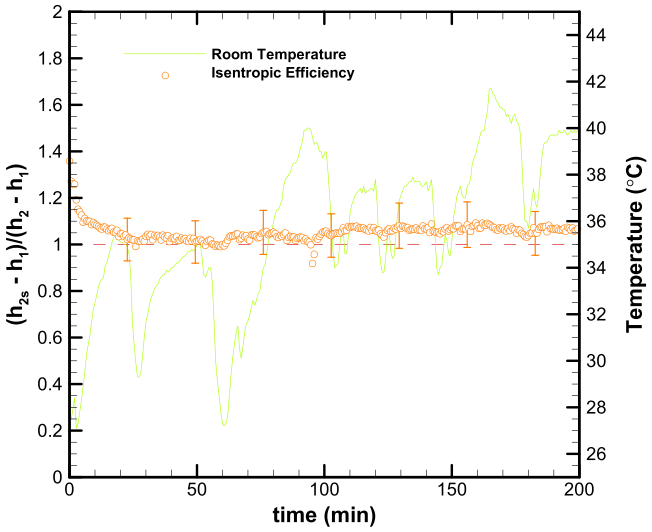

Fig. 4. Apparent isentropic efficiency for air-cooled swashplate compressor.

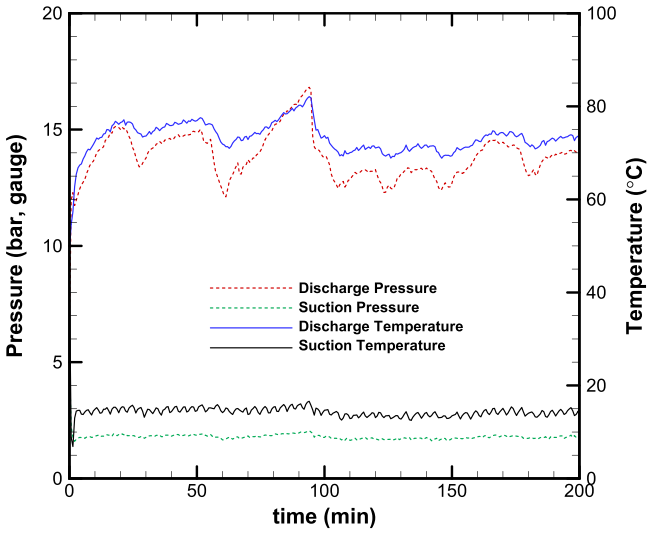

Fig. 5. Temperature and pressure conditions corresponding to Fig. 4.

3.3. Effect of cooling fan speed

The effect of cooling fan speed on the compressor performance as a measure of IPC was also captured while keeping supply and discharge lines pressure constant. As listed in Table 4, higher fan velocity leads to increased isentropic performance coefficient by 0.06. This is consistent with the explanation that intentional cooling of the compressor can improve the apparent isentropic efficiency. The power consumption was almost same for both cases.

4. Discussion

4.1. Using compressor power input to calculate η_s

A second way to determine the isentropic efficiency of an electric compressor is to use measured power input and work from the definition:

$$\eta_s = \frac{\dot{W}_s}{\dot{W}_a} \tag{4}$$

If $\dot{W}_a$ is taken to be the electrical power input rather than shaft power going into the compressor, a considerably lower isentropic efficiency results than the value calculated from the enthalpies (Eq. 3). This is because the efficiency of the electric motor plays a role. For the current compressor, the electric motor efficiency is 80–90% depending on load and rpm. This will drop the isentropic efficiency reported in Table 1 from 104% to as low as 83%. The value would be even lower again if we also included the electrical power to run condenser fans.

4.2. Ultimate performance measure of a cooled refrigeration compressor

Having established experimentally that the apparent isentropic efficiency can exceed 100% through cooling, it is interesting to consider upper limits on performance enhancement through cooling a refrigeration compressor. Note that this is different to an air compressor where isothermal compression would be the upper limit. In the case of a refrigeration compressor, we also need to avoid the appearance of the liquid phase in the compressor. Moreover, cooling without evaporation is limited to the ambient temperature. Thus, the path during compression must be considered.

As illustrated by Fig. 1b) and c), the path to reducing the compressor discharge temperature has an important role in terms of the compressor power input. If heat is removed after the compression process (Fig. 1b), the only benefit is the reduced load on the condenser. If heat is removed

Table 3
Effect of compressor speed.

RPM	*T_{suc} (º C)*	*P_{suc} (Bar)*	*h_{vap} (kJ/kg)*	*s (kJ/kg.K)*	*$T_{dis,\ isen}$ (º C)*	*T_{dis} (º C)*	*P_{dis} (Bar)*	*P_{comp} (kW)*	*IPC*
996	25.8	3.9	392.95	1.717	77.8	76.1	18.5	2.1	1.06
1848	22.78	3.8	390.29	1.711	75.8	77.7	18.5	3.5	0.93

Table 4
Effect of cooling fan speed (R404a).

RPM	Fan RPM	T_{suc} (º C)	P_{suc} (Bar)	T_{dis} (º C)	P_{dis} (Bar)	P_{comp} (kW)	IPC
1848	6696	13.7	1.86	81.2	15.1	3.9	0.95
1848	0	14.4	1.86	79.4	15.1	3.9	0.89

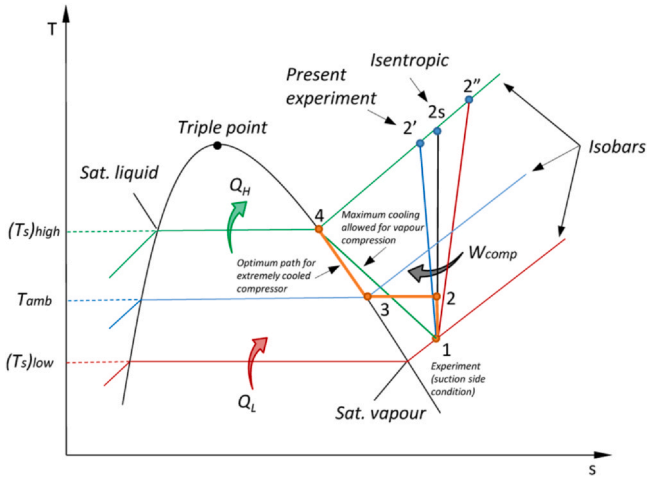

Fig. 6. T-s diagram showing optimum path (*1–2-3–4*) for cooled refrigeration compressor.

during the compression process (Fig. 1c) the compressor work input is reduced. This can be seen in the T-s diagram given in Fig. 6. Here, *2'* represents the condition at the outlet of the air-cooled compressor with apparent isentropic efficiency greater than 100%. If the path is directly from *1* to *2'* then compressor work is reduced. If on the other hand, the path is *1 → 2" → 2'* then the compressor work will be similar to the adiabatic compressor (Fig. 1a).

For intentionally cooled refrigeration compressors, it is worth considering the ultimate possible gains through removal of heat during compression. If we have the additional requirement that the refrigerant must always remain a vapour, then evidently the point 4 on the discharge isobar shown in Fig. 6 would be the limit to which cooling could be permitted. Since external cooling cannot take place for temperatures lower than the ambient, the best possible path to get to point *4* would be *1→ 2→ 3→ 4* shown by the orange line in Fig. 6.

The work done per kg of refrigerant along the various paths can be determined from Eqs. (5–10):

$$W_{2-3} = h_3 - h_2 + \int_3^2 Tds \tag{5}$$

$$W_{3-4} = h_4 - h_3 + \int_4^3 Tds \tag{6}$$

Table 5
Work saving through optimum path.

T_{amb} (º C)	Mass flow rate (kg/s)	$(Tds)_{2-3}$ kJ/kg	$(Tds)_{3-4}$ kJ/kg	$(W)_{1-4}$ kJ/kg	$(W)_{1-2s}$ kJ/kg	Saving (%)
26.6	0.0923	18.46	3.29	35.09	37.66	**6.8%**

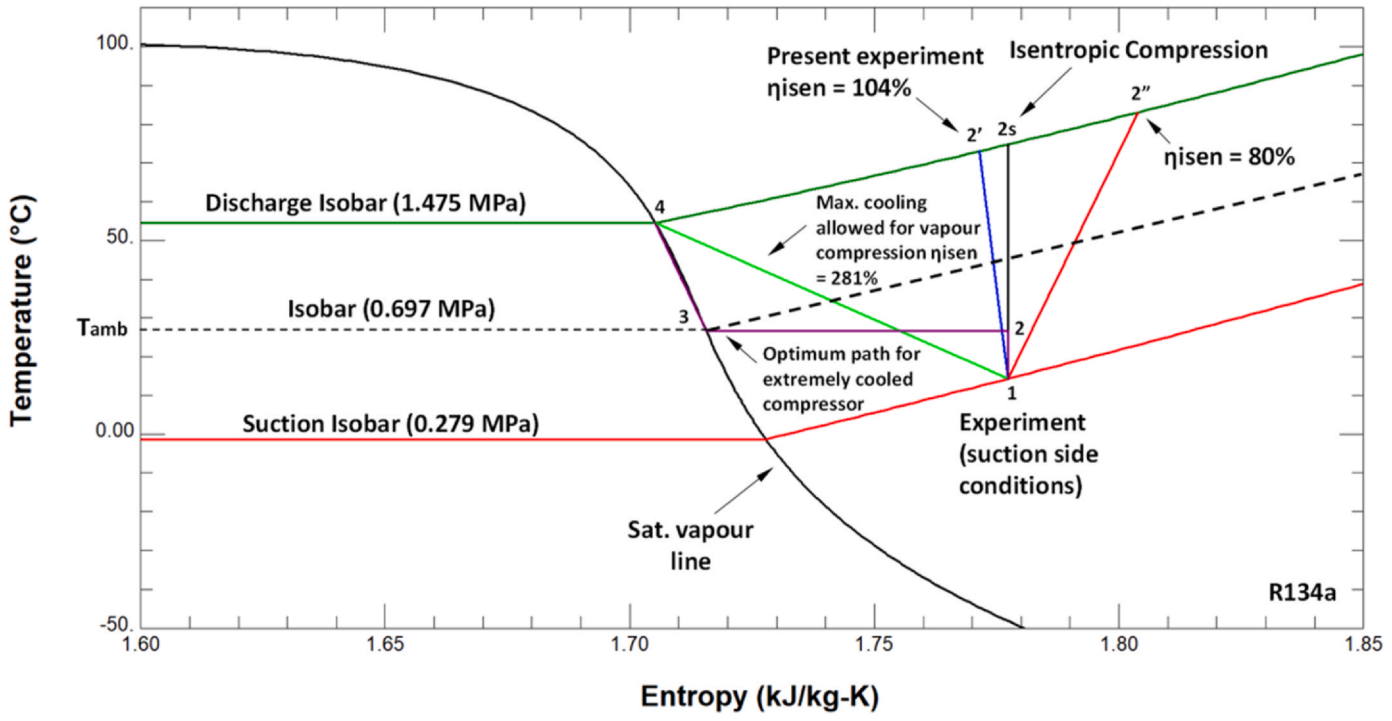

Fig. 7. T-s diagram showing optimum path (1 – 2-3 – 4) for extremely cooled refrigeration compressor.

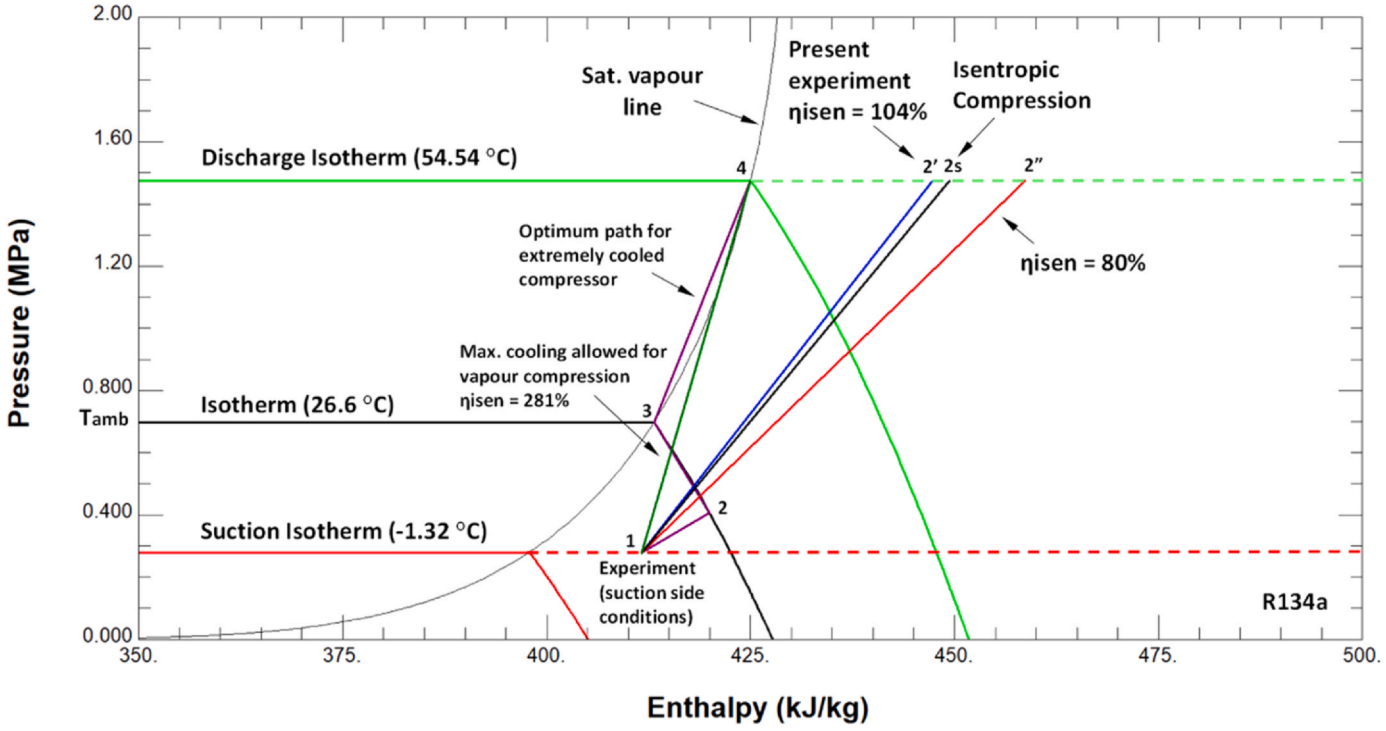

Fig. 8. P-h diagram showing optimum path (1 − 2-3 − 4) for extremely cooled refrigeration compressor.

$$\int_{s3}^{s2} Tds = \quad T_{amb}(s_2 - s_3) \tag{7}$$

$$\int_{s4}^{s3} Tds \cong 0.5(T_4 + T_3) \quad (s_3 - s_4) \tag{8}$$

$$W_{1-4} = (h_4 - h_1) + \int_4^1 Tds \tag{9}$$

$$W_{1-2s} = h_{2s} - h_1 + \int_4^{2s} Tds \tag{10}$$

Table 5 illustrates the possible saving in work through taking the path *1→ 2→ 3→ 4* compared with isentropic compression for the isobars and compressor inlet superheat listed in Table 1. 2.57 kJ/kg of refrigerant represents a saving of 6.8% compared with isentropic compression. The T-s and P-h diagrams for R134a for this case are shown in Figs. 7 and 8.

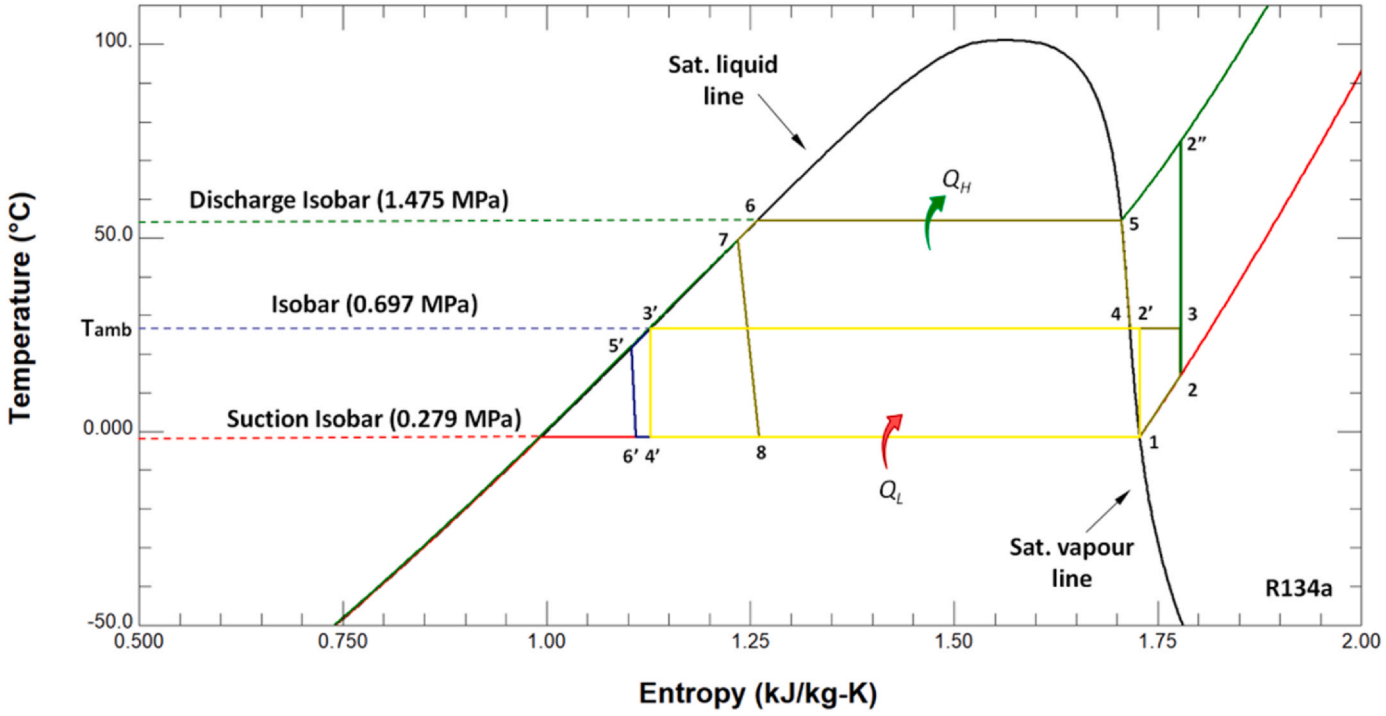

Fig. 9. T-s diagram showing optimum path (2–3-5'-6'-2) for extremely cooled refrigeration compressor.

Table 6
Performance analysis of different cycles shown in Fig. 9.

Cycle	W_C *(kJ/kg)*	Q_H *(kJ/kg)*	Q_L *(kJ/kg)*	*COP*	*Equations used*
I (2–2”-6–7–8–2)	37.66	178.46	140.8	3.73	$W_c = (h_{2'} - h_2) \quad Q_H = (h_{2'} - h_7) \quad Q_L = (h_2 - h_8) \quad COP = \frac{Q_L}{W_c}$
II (2 – 3 – 4 – 5 – 6 – 7 – 8 – 2)	35.09	154.16	140.8	4.01	$W_c = (h_5 - h_2) + \int_{s5}^{s2} Tds \quad Q_H = (h_5 - h_7) \quad Q_L = (h_2 - h_8) \quad COP = \frac{Q_L}{W_c}$
III (2–3–3’-5’-6’-2)	26.77	183.41	181.91	6.79	$W_c = (h_3 - h_2) + \int_{s4}^{s3} Tds \quad Q_H = (h_4 - h_{5'}) \quad Q_L = (h_2 - h_{6'}) \quad COP = \frac{Q_L}{W_c}$
IV (1–2’-3’-4’-1)	16.76	179.94	163.17	9.73	$W_c = (T_{amb} - T_{suc})(s_1 - s_{4'}) \quad Q_H = T_{amb}(s_{2'} - s_{3'}) \quad Q_L = T_{suc}(s_1 - s_{4'}) \quad COP = \frac{Q_L}{W_c}$

4.3. Impact limits of intentional cooling of compressor on COP of refrigeration circuit

Since a refrigerant compressor serves the purpose of driving a refrigeration circuit, it is worthwhile considering the upper limits to the coefficient of performance of a refrigeration circuit with intentional cooling of the compressor. Fig. 9 extends Fig. 7 to include the whole vapour-liquid refrigeration cycle. The path 2–2”-6–7–8–2 (listed as **I** in Table 7) represents the standard ideal path with isentropic compression. This path has a COP of 3.73 for the given isobars, suction superheat and 5 K subcooling of the liquid refrigerant exiting the condenser. If the compression occurs along the proposed path **II** (2 – 3 – 4 – 5 – 6 – 7 – 8 – 2), the COP increases to 4.01. This shows that the best possible improvement to the COP by cooling the refrigeration compressor is only about 7.5% (relative to an isentropic compressor) for the case considered.

To achieve a really substantial improvement to the COP by cooling, the restriction of not allowing the refrigerant to condense into a liquid during compression would need to be lifted. This is illustrated by path **III** (2–3–3’-5’-6’-2) in Fig. 9 and Table 6. For this case the COP is 6.79 which represents an 82% improvement and is becoming comparable to the Carnot refrigerator (path **IV** (1–2’-3’-4’-1)) which has a COP of 9.73.

5. Conclusions

In this article we have focused on the effects of intentional cooling during the compression process for an air-cooled swashplate refrigeration compressor. Experimental results show surprisingly high apparent isentropic efficiencies if calculated based on the enthalpies from measured suction and discharge temperatures and pressures. Under some conditions, the apparent isentropic efficiency may became greater than unity which we showed was possible with external cooling. Conventional wisdom suggests the isentropic efficiency has no meaning for intentionally cooled compressors, however we argue that it is still a useful measure for comparison since a compressor with a reduced discharge temperature is functionally a better compressor. To overcome the possible counterintuitive ‘isentropic efficiency’ of greater than 100% we suggest that for cases of intentional compressor cooling, the simple definition for isentropic efficiency is retained as a performance measure but renamed to isentropic performance coefficient (IPC). For a refrigeration compressor, the ultimate performance improvement through cooling the compression process is severely limited by the requirement that the refrigerant must remain a vapour. If this restriction did not exist, and the bulk of the compression was done in an isothermal two-phase process at ambient temperature, then the COP of the resulting refrigeration cycle would approach the COP of the Carnot refrigerator.

CRediT authorship contribution statement

Mohammad Arqam: Writing – review & editing, Writing – original draft, Methodology, Investigation, Data curation, Conceptualization. **Amir Jahangiri:** Writing – review & editing, Validation. **Mark Mitchell:** Writing – review & editing, Supervision, Project administration. **Nick S. Bennett:** Writing – review & editing, Visualization. **Peter Woodfield:** Writing – review & editing, Writing – original draft, Supervision.

Data Availability

Data will be made available on request.

Declaration of Competing Interest

The authors declare that they have no known competing financial interests or personal relationships that could have appeared to influence the work reported in this paper.

Acknowledgement

This study was co-funded by the department of Industry, (Innovation and Science (Innovative Manufacturing CRC Ltd) SuperCool Asia Pacific Pty Ltd (IMCRC/SCL/010917). Special thanks to **Daniel Brown (Engineer)** at SuperCool Asia Pacific Pty. Ltd. Ormeau, QLD, Australia for assisting in testing and experiments.

References

[1] M. Arqam, D.V. Dao, A. Jahangiri, H. Yan, M. Mitchell, P.L. Woodfield, Analytical model for a 10 cylinder swash plate electric compressor, ASHRAE Trans. *126* (2020) 351–359.
[2] M. Arqam, D.V. Dao, A. Jahangiri, M. Mitchell, P. Woodfield, Real gas model for an electric swashplate refrigeration compressor, Int. J. Refrig. *118* (2020) 210–219.
[3] M. Arqam, D.V. Dao, M. Mitchell, P. Woodfield, Transient start-up of an electric swashplate refrigeration compressor, Appl. Thermal Eng. 196 (2021) 117351.
[4] S.Y. Sun, T.R. Ren, New method of thermodynamic computation for a reciprocating compressor: computer simulation of working process, Int. J. Mechan. Sci. *37* (4) (1995) 343–353.
[5] M. Farzaneh-Gord, A. Niazmand, M. Deymi-Dashtebayaz, H.R. Rahbari, Effects of natural gas compositions on CNG (compressed natural gas) reciprocating compressors performance, Energy *90* (2015) 1152–1162.
[6] M. Farzaneh-Gord, A. Niazmand, M. Deymi-Dashtebayaz, H.R. Rahbari, Thermodynamic analysis of natural gas reciprocating compressors based on real and ideal gas models, int. J. refrig. *56* (2015) 186–197.
[7] M. Farzaneh-Gord, S. Izadi, S.I. Pishbin, H. Sheikhani, M. Deymi-Dashtebayaz, Thermodynamic analysis of medium pressure reciprocating natural gas expansion engines, Polish J. Chem.Technol. *17* (2) (2015) 119–125.
[8] M.F. Gord, M. Jannatabadi, Simulation of single acting natural gas Reciprocating Expansion Engine based on ideal gas model, J. Natural Gas Sci. Eng. *21* (2014) 669–679.
[9] M. Farzaneh-Gord, H. Khoshnazar, Valve fault detection for single stage reciprocating compressors, J. Nat. Gas Sci. Eng. *35* (2016) 1239–1248.
[10] B. Yang, C.R. Bradshaw, E.A. Groll, Modeling of a semi-hermetic CO2 reciprocating compressor including lubrication submodels for piston rings and bearings, Int. J. Refrig. *36* (7) (2013) 1925–1937.
[11] T. Dutra, C.J. Deschamps, A simulation approach for hermetic reciprocating compressors including electrical motor modeling, Int. J. Refrig. *59* (2015) 168–181.
[12] T. Wang, Z. He, J. Guo, X. Peng, Investigation of the Thermodynamic Process of the Refrigerator Compressor Based on the m-θ Diagram. Energies *10* (10) (2017) 1517.
[13] B. Zhao, X. Jia, Y. Zhang, J. Feng, X. Peng, Investigation on transient temperature of a reciprocating compressor based on a two-thermocouple probe, Int. J. Thermal Sci. *122* (2017) 313–325.

[14] M. Elhaj, F. Gu, A.D. Ball, A. Albarbar, M. Al-Qattan, A. Naid, Numerical simulation and experimental study of a two-stage reciprocating compressor for condition monitoring, Mechan. Syst. Signal Process. *22* (2) (2008) 374–389.
[15] E. Winandy, C. Saavedra, J. Lebrun, Simplified modelling of an open-type reciprocating compressor, Int. J. Thermal Sci. *41* (2) (2002) 183–192.
[16] D. Ndiaye, M. Bernier, Dynamic model of a hermetic reciprocating compressor in on–off cycling operation (Abbreviation: Compressor dynamic model), Appl. Thermal Eng. *30* (8-9) (2010) 792–799.
[17] P. Stouffs, M. Tazerout, P. Wauters, Thermodynamic analysis of reciprocating compressors, Int. J.Thermal Sci. *40* (1) (2001) 52–66.
[18] J. Rigola, C.D. Perez-Segarra, A. Oliva, Parametric studies on hermetic reciprocating compressors, Int. J. Refrig. *28* (2) (2005) 253–266.
[19] J. Castaing-Lasvignottes, S. Gibout, Dynamic simulation of reciprocating refrigeration compressors and experimental validation, Int. J. Refrig. *33* (2) (2010) 381–389.
[20] D. Roskosch, V. Venzik, B. Atakan, Thermodynamic model for reciprocating compressors with the focus on fluid dependent efficiencies, Int. J. Refrig. *84* (2017) 104–116.
[21] S. Posch, J. Hopfgartner, E. Berger, B. Zuber, P. Schöllauf, R. Almbauer, Numerical analysis of a hermetic reciprocating compressor oil pump system, Int. J. refrig. *85* (2018) 135–143.
[22] E. Navarro, E. Granryd, J.F. Urchueguía, J.M. Corberán, A phenomenological model for analyzing reciprocating compressors, Int. J. Refrig. *30* (7) (2007) 1254–1265.
[23] M. Farzaneh-Gord, A. Niazman, M. Deymi, Optimizing reciprocating air compressors design parameters based on first law analysis, UPB Sci. Bull. Seriese D: Mech. Eng. (2013) 13–26.
[24] J.A. McGovern, S. Harte, An exergy method for compressor performance analysis, Int. J. Refrig. *18* (6) (1995) 421–433.
[25] C. Aprea, R.I.T.A. Mastrullo, C. Renno, Determination of the compressor optimal working conditions, Appl. Thermal Eng. *29* (10) (2009) 1991–1997.
[26] T. Bin, Z. Yuanyang, L. Liansheng, L. Guangbin, W. Le, Y. Qichao, ... M. Wenhui, Thermal performance analysis of reciprocating compressor with stepless capacity control system, Appl. Thermal Eng. *54* (2) (2013) 380–386.
[27] A. Morriesen, C.J. Deschamps, Experimental investigation of transient fluid flow and superheating in the suction chamber of a refrigeration reciprocating compressor, Appl. Thermal Eng. *41* (2012) 61–70.
[28] B. Yang, C.R. Bradshaw, E.A. Groll, Modeling of a semi-hermetic CO2 reciprocating compressor including lubrication submodels for piston rings and bearings, Int. J. Refrig. *36* (7) (2013) 1925–1937.
[29] Y.A. Cengel, M.A. Boles, M. Kanoğlu, Thermodynamics: an engineering approach Vol. 5 McGraw-hill, New York, 2011, p. 445.
[30] Z. Zou, P. Xu, C. Fu, An evaluation model for wall heat transfer effects on micro centrifugal compressors and its application in aerodynamic design, Appl. Thermal Eng. *236* (2024) 121554.
[31] E.W. Lemmon, M.L. Huber, M.O. McLinden, version, NIST standard reference database 23. *Reference fluid thermodynamic and transport properties ((((REFPROP)))) 9* (2010).